

ANGPT1 promotes M1 macrophage polarization and inhibits lung adenocarcinoma progression by inhibiting the TGF- β signalling pathway

Gang Liu^{1,2} and Hao Zhang^{1,3} 

¹ Department of Thoracic Surgery, The Affiliated Hospital of Xuzhou Medical University, Xuzhou City, Jiangsu Province, China

² Department of Thoracic Surgery, The Second Affiliated Hospital of Bengbu Medical University, Bengbu City, Anhui Province, China

³ Thoracic Surgery Laboratory, Xuzhou Medical University, Xuzhou City, Jiangsu Province, China

Abstract. Immune cells in the immune microenvironment of lung adenocarcinoma (LUAD) are involved in tumour progression. The aim of this study was to investigate the molecular mechanisms of immune infiltration-related genes in LUAD. The GEO, GeneCards, BioGPS and Genehopper databases were utilized to screen for immune infiltration-related differentially expressed genes (DEGs) in LUAD. Protein-protein interaction (PPI) network construction and survival analysis were performed in the Kaplan-Meier database to identify hub genes. The TIMER 2.0 database was used to analyse the correlations between hub gene expression and immune infiltration level. Co-culture of LUAD cells with macrophages and plasmid transfection to overexpress ANGPT1 were performed to investigate the function of the hub genes in LUAD using RT-qPCR, Western blot, CCK-8 assays, cell wound healing assays and transwell assays. A total of 88 immune infiltration-related DEGs were screened. The hub genes *ANGPT1*, *CDH5* and *CLDN5* were reduced in LUAD, while *COL3A1* was overexpressed. *ANGPT1* was significantly correlated with OS, FP and PPS, and *ANGPT1* promoted the polarization of M1 macrophages. Further experiments revealed that *ANGPT1* inhibited the proliferation, migration and invasion of LUAD cells by inhibiting the TGF- β signalling pathway. *ANGPT1* promotes polarization of M1 macrophages and reduces the progression of LUAD by inhibiting the TGF- β signalling pathway. Thus, *ANGPT1* could be employed as a predictive biomarker and immunotherapy target for lung cancer.

Key words: Lung adenocarcinoma — Immune infiltration — *ANGPT1* — TGF- β signalling pathway

Introduction

Lung adenocarcinoma (LUAD) is a prevalent subtype of lung cancer associated with a high mortality rate; it accounts for almost 40% of all cases of lung cancer (Travis et al. 2011; Hutchinson et al. 2019). LUAD is characterized by significant

heterogeneity and aggression (Zhang et al. 2020). The main treatment options for LUAD include surgery, radiotherapy and molecular therapeutics. However, the five-year survival rate of patients remains relatively low (Zhang et al. 2019; Jurisic et al. 2020). Increasing evidence suggests that immunotherapy has contributed to improved survival among patients with LUAD (Spella and Stathopoulos 2021). Therefore, it is important to explore the targets of immunotherapy for LUAD.

Tumour-infiltrating immune cells (TIICs), a crucial component of the tumour microenvironment (TME), significantly impact immunotherapy (Amaral et al. 2018). TIICs mainly include B lymphocytes, T lymphocytes, tumour-

Electronic supplementary material. The online version of this article (doi: 10.4149/gpb_2024001) contains Supplementary material.

Correspondence to: Hao Zhang, Department of Thoracic Surgery, The Affiliated Hospital of Xuzhou Medical University, No. 99, West Huaihai Road, Xuzhou City, Jiangsu Province, 221006, China
E-mail: zhanghao_xz667@163.com

associated macrophages (TAMs), dendritic cells, neutrophils and natural killers (Chen et al. 2020). Much effort has been directed into the development of immunotherapies based on TIICs. Among them, TAMs exhibit remarkable plasticity and can effectively clear tumour cells and modulate the adaptive immune system *via* reprogramming, making them a promising target for cancer immunotherapy (Liu et al. 2021). In LUAD, targeting *USP7* has been shown to reprogram TAMs and enhance the anti-tumour immune response (Dai X et al. 2020). The identification of macrophage-related molecular subtypes of LUAD has revealed novel TMEs that have significant prognostic and therapeutic implications (Wen et al. 2022). The expression levels of clinical M2 macrophage-related genes have been shown to be dependable predictors of LUAD and may serve as effective clinical indicators (Xu et al. 2022). Therefore, further exploration of the correlations between immune infiltration-related genes and macrophages in LUAD is crucial.

Angiopoietin-1 (*ANGPT1*) encodes a secreted glycoprotein of the angiopoietin family and is essential for vascular development and angiogenesis (Suri et al. 1996). *ANGPT1* acts as an agonist of *Tie2* and plays a significant role in tumour vessel maturation (Jayson et al. 2016). The activation of *Tie2* receptors by *ANGPT1* promotes the maturation of blood vessels in squamous cell carcinoma and inhibits tumour growth (Hawighorst et al. 2002). In terms of immunotherapy, inhibiting *ANGPT1* and *Tie2* can modulate immunogenicity in breast, colon and prostate cancers and enhance the sensitivity of human tumour cells to immune attack (Grenga et al. 2015). However, the specific molecular mechanism and role of *ANGPT1* in LUAD remain unclear.

The aim of this study was to explore the role and mechanism of immune infiltration-related genes in LUAD and provide a theoretical basis for LUAD immunotherapy. To achieve this, immune infiltration-related differentially expressed genes (DEGs) in LUAD were screened using the Gene Expression Omnibus (GEO) database in conjunction with the GeneCards, BioGPS and Genehopper databases. Then, functional enrichment analysis of the DEGs was performed. Ultimately, *ANGPT1* was identified as a prognostic factor related to immunological infiltration. Further, through *in vitro* experiments using A549 and H1299 cells, the role and molecular mechanism of *ANGPT1* were investigated.

Materials and Methods

Microarray data source

The GSE7670 and GSE63459 datasets were acquired from the GEO database (<https://www.ncbi.nlm.nih.gov/geo/>).

Specific details on the above datasets are presented in Table S1 (in Supplementary material).

Screening for immune-related DEGs

DEGs from the GSE7670 and GSE63459 datasets were identified using GEO2R (<https://www.ncbi.nlm.nih.gov/geo/geo2r>) based on the criteria of $p\text{-adj} < 0.05$ and $|\log\text{FC}| \geq 2$. The keyword “immune infiltration” was used to identify related genes in the GeneCards (<https://www.genecards.org/>), BioGPS (<http://biogps.org/#goto=welcomed>) and Genehopper (<http://genehopper.ifis.cs.tu-bs.de/>) databases. DEGs related to immune infiltration that were common to both datasets were identified through the use of a Venn diagram (<http://jvenn.toulouse.inra.fr/app/example.html>). In addition, DEGs are visualized by volcano plots and heatmaps using the ggplot2 and pheatmap packages in the R software (version 4.1.3).

Functional enrichment analysis

Functional enrichment analysis of the Gene Ontology (GO) database, including molecular function (MF), biological process (BP) and cellular component (CC), and the Kyoto Encyclopaedia of Genes and Genomes (KEGG) pathways was performed for the overlapping DEGs using the Database for Annotation, Visualization, and Integrated Discovery (DAVID) (<https://david.ncifcrf.gov/>). The GO and KEGG enrichment analysis plots were generated using the tools provided on the Bioinformatics website (<http://www.bioinformatics.com.cn/login/>).

PPI network construction and hub module analysis

To investigate the relationships between the DEGs, a protein-protein interaction (PPI) network was constructed using the STRING database (<https://cn.string-db.org/>), with a confidence score of 0.4 as the threshold. Within the PPI network, the hub modules were identified using the molecular complex detection (MCODE) plug-in in Cytoscape software (version 3.9.1). The screening criteria were as follows: degree cutoff = 2, node score cutoff = 0.2, K-core = 2, and max depth = 100.

Validation of hub gene expression profiles and analysis of GO enrichment in databases

A circle plot of the GO enrichment of the 16 hub genes was generated using the clusterProfiler, enrichplot and ggplot2 packages in the R software. The mRNA expression levels of the hub genes *ANGPT1*, *CDH5*, *CLDN5* and *COL3A1* were analysed in the GEPIA database (<http://gepia.cancer-pku.cn/index.html>).

Survival analysis of the hub genes

The Kaplan-Meier plotter database (<http://kmplot.com/analysis/>) is a valuable tool for gene prognostic analysis, drawing data from the European Genome-Phenome Archive (EGA), the GEO, and the Cancer Genome Atlas (TCGA, <http://cancergenome.nih.gov>) cancer datasets (Gyorffy et al. 2013). In our study, we utilized the Kaplan-Meier plotter database to explore the correlations between the expression levels of hub genes and overall survival (OS), first progression survival (FP), and post-progression survival (PPS) in LUAD. A total of 1161 LUAD patients were included for OS analysis, 906 patients for FP analysis, and 376 patients for PPS analysis. Additionally, receiver operating characteristic (ROC) curves were generated using the pROC package in the R software to explore the possibility of *ANGPT1* as a biomarker for LUAD.

Correlation analysis between *ANGPT1* and TIICs

The relationship between *ANGPT1* expression and CD8+T cell immune infiltration across different tumours was investigated using the TIMER 2.0 database (<http://timer.cistrome.org/>). This relationship was further analysed in LUAD with a focus on various immune cell infiltrations within the TME. This analysis was performed using a specific tool available on the same website (<https://cistrome.shinyapps.io/timer/>).

Cell culture

The human normal lung epithelial cell line BEAS-2B and the lung cancer cell lines A549 and H1299 (Icellbioscience, Shanghai, China) were grown in RPMI-1640 medium with 100 U/ml penicillin, streptomycin (Thermo Fisher Scientific, New York, USA) and 10% foetal bovine serum. All cells were cultured at 37°C in an environment of 5% CO₂ and 95% humidity.

Cell transfection

The pcDNA-*ANGPT1* plasmid, designed to overexpress *ANGPT1*, was created by cloning the *ANGPT1* coding sequence into the pcDNA3.1 vector. Both H1299 and A549 cells were transfected with the pcDNA-*ANGPT1* plasmid using Lipo6000™ (Beyotime, Shanghai, China), with the empty pcDNA-NC plasmid serving as a negative control. For *in vitro* cellular assays, the TGF-β signalling pathway activator SRI-011381 (MedChemExpress, catalogue number: HY-100347) was added to the cells at a concentration of 10 μM.

LUAD cells and macrophage co-culture

LUAD cells and macrophages were co-cultured in a Transwell® non-contact co-culture system (#3450, Corning,

USA). Human macrophages were derived from THP-1 monocytes. To generate macrophages, 1×10⁶ THP-1 cells (Icellbioscience) were inoculated into the bottom chamber of a cell culture insert supplemented with RPMI-1640 medium containing 10 ng/ml 12-carnitine 13-acetate (PAM, Sigma). Twenty-four hours later, the initial medium was changed to PRIM-1640 medium, and lung cancer cells overexpressing *ANGPT1* were inoculated into the higher chamber and co-cultured with macrophages for 72 h. THP-1-derived primary macrophages (M0) were used as a control.

RNA extraction and real-time quantitative PCR (RT-qPCR)

Total RNA was extracted from the cultured cells using TRIzol reagent (Thermo Fisher Scientific, Shanghai, China). cDNA synthesis was performed using a Hiscript II QRT Supermix Reverse Transcription Kit (Vazyme Medical). The cDNA samples were then evaluated by qPCR using the SYBR method. The level of gene expression was determined using the 2^{-ΔΔCt} comparative method. The sequences of the primers are provided in Table S2 (see Supplementary material).

Western blot

RIPA buffer containing protease inhibitors was used to lyse the total proteins. The extracted proteins were separated with 10% SDS-PAGE and then transferred to polyvinylidene fluoride (PVDF) membranes (Roche, Basel, Switzerland). The PVDF membranes were covered with 5% defatted milk powder for 2 h at room temperature. The primary antibodies, including anti-*iNOS* (Abcam, Cambridge, UK), anti-*CD206* (Abcam), anti-*TGF-β* (Abcam), anti-*Smad2* (Abcam), anti-p-*Smad2* (Abcam), anti-*Smad3* (Abcam), anti-p-*Smad3* (Abcam), and secondary antibodies (Abcam) were diluted with fresh 5% defatted milk powder at a ratio of 1:2000 and 1:5000, respectively. The target protein bands were developed with ECL luminescent solution (Amersham, Little Chalfont, UK) and quantitatively analysed by ImageJ software.

CCK-8

First, 100 μl of cell suspension (with a cell density of 4×10⁵/ml) was added to each well of a 96-well plate. At 0, 24, 48, 72, and 96 h, 10 μl of CCK-8 solution (Solarbio) was added to each well and the cells were incubated in the dark for 2 h. The absorbance at 450 nm was measured using a microplate reader (DALB, Shanghai, China).

Cell wound healing assay

Cells were seeded in six-well plates at a density of 1×10⁵/ml. Once the cell density reached 80% or more, a straight line

was scratched into the monolayer using a pipette tip, initiating the wound healing assay. The cells were then cultured in serum-free RPMI-1640 medium. Images were captured at 0 and 24 h, and the cell migration ability was analysed using ImageJ software.

Transwell assay

Cells were seeded at a density of 5×10^5 /ml in six-well plates containing Transwell inserts with 8 μ m pores. The upper chamber was filled with 100 μ l of serum-free RPMI-1640 medium, while the lower chamber was filled with 600 μ l of medium containing 10% FBS. After incubation, the cells were fixed with 4% paraformaldehyde for 30 min and then stained with 0.1% crystal violet.

Statistical analysis

Statistical analysis was performed using GraphPad Prism 9 (version 9.5.0.730). Student's *t*-tests were used to compare two groups while Tukey's test-corrected one-way analysis of variance (ANOVA) was used for comparisons of more than two groups. $p < 0.05$ was considered statistically significant.

Results

Identification of immune infiltration-associated DEGs

Firstly, the read counts for each sample in the GSE7670 and GSE63459 datasets were normalized, and the findings showed a high level of consistency in the median values across all samples, which indicated that both two datasets met the criteria for further investigation (Fig. S1 in Supplementary material). The bioinformatics analysis identified 287 DEGs in the GSE7670 dataset and 408 DEGs in the GSE63459 dataset (Fig. 1A). The top 20 DEGs in the GSE7670 and GSE63459 datasets are listed in Table S3 (in Supplementary material). Among both datasets, we selected the top 50 DEGs for cluster analysis from each sample, including the 10 samples with the most significant differential expression (Fig. 1B and Fig. S2 in Supplementary material). The Venn diagram results revealed the presence of 124 overlapping DEGs in the GSE7670 and GSE63459 datasets. Then, the 124 overlapping DEGs were intersected with the immune infiltration dataset. In total, 88 overlapping DEGs associated with immune infiltration in LUAD were identified (Fig. S3 in Supplementary material).

Functional enrichment analysis of DEGs

GO and KEGG pathway enrichment analysis of the overlapping DEGs was performed in the DAVID database to

investigate the possible biological roles of these DEGs in LUAD. The top six GO terms were selected based on their $-\log_{10}$ (p value). GO enrichment analysis of BP indicated that the DEGs were primarily associated with elastic fibre components. For CC, the DEGs were related to collagen fibre tissue. For MF, the DEGs were mainly involved in transforming growth factor- β (TGF- β) activity (Fig. 2A). Figure 2B shows the top 25 KEGG pathways, ranked by their $-\log_{10}$ (p value). The results indicated that the DEGs were mainly involved in the malaria, protein digestion and absorption, and extracellular matrix (ECM) receptor interaction.

Construction of a PPI network and analysis of the hub genes

After analysis in the STRING database, the DEGs were entered into Cytoscape software to construct the PPI network. The MCODE plug-in was used to filter out the three modules with the highest relationship (Fig. 3A). The highest-scoring module scored 5.733, with 16 points and 43 edges, and included 16 genes. Then, the 16 genes in the highest-scoring modules were selected as hub genes for subsequent analysis (Fig. 3B).

GO enrichment analysis and mRNA expression analysis of the hub genes

GO analysis revealed that the 16 hub genes were primarily involved in ECM organization, collagen degradation, and the PI3K-Akt-mTOR and TGF- β pathways (Fig. S4 in Supplementary material). Subsequently, by reviewing the relevant literature, among the 16 key genes, *ANGPT1*, *CDH5*, *CLDN5* and *COL3A1* were selected for further analysis, which aroused our great interest due to the fact that they have not been extensively studied in LUAD. Subsequently, the mRNA expression levels of these hub genes were examined using GEPIA. The results revealed that *ANGPT1*, *CDH5* and *CLDN5* were substantially downregulated, whereas *COL3A1* was substantially upregulated compared with normal samples (Fig. 4A). Survival analysis revealed significant correlations between OS in LUAD and the genes *ANGPT1*, *CDH5*, *CLDN5* and *COL3A1* (Fig. 4B). Only *ANGPT1* was significantly correlated with OS, FP and PPS (Fig. 4C,D). Therefore, *ANGPT1* was selected as the focus for subsequent studies.

Survival and immune infiltration analysis of ANGPT1 in LUAD

The ROC curve of *ANGPT1* expression was constructed and analysed using R software. With an AUC value of 0.706, *ANGPT1* demonstrated potential as a prognostic indicator for LUAD (Fig. 5A). Then, the analysis of im-

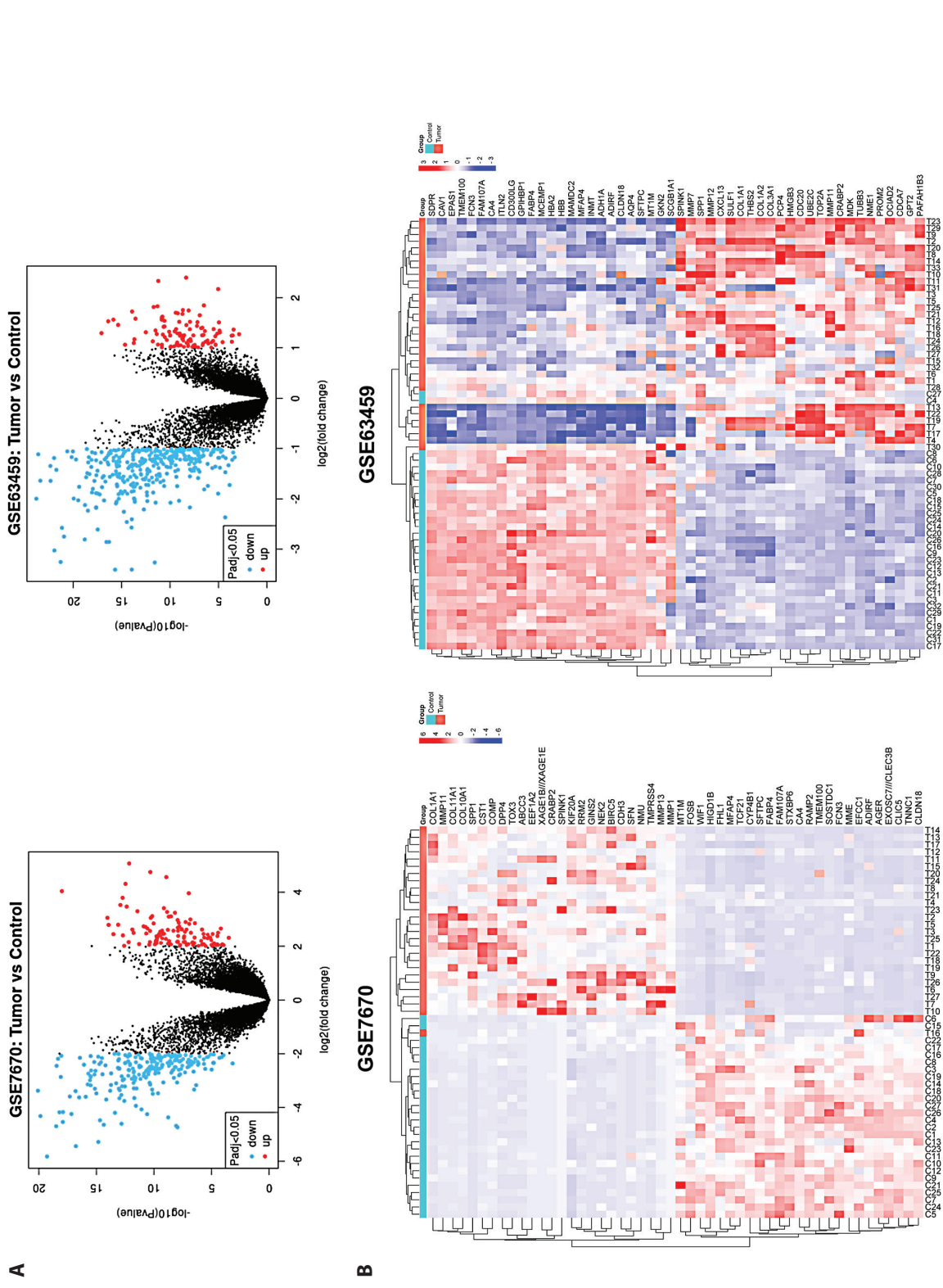


Figure 1. Screening of DEGs in the GSE7670 and GSE63459 datasets according to $p\text{-adj} < 0.05$ and $|\log_{2}FC| \geq 2$. **A.** Volcano map of DEGs in the GSE7670 and GSE63459 datasets. The abscissa represents $\log_2(\text{fold change})$ and the ordinate represents $-\log_{10}(p\text{ value})$. The red dots represent the up-regulated genes, the blue dots represent the down-regulated genes, and the black dots represent the non-significant DEGs. **B.** Heatmap of the top 50 ranked DEGs. Red represents genes with high expression and blue represents genes with low expression. For color figure see online version of the article.

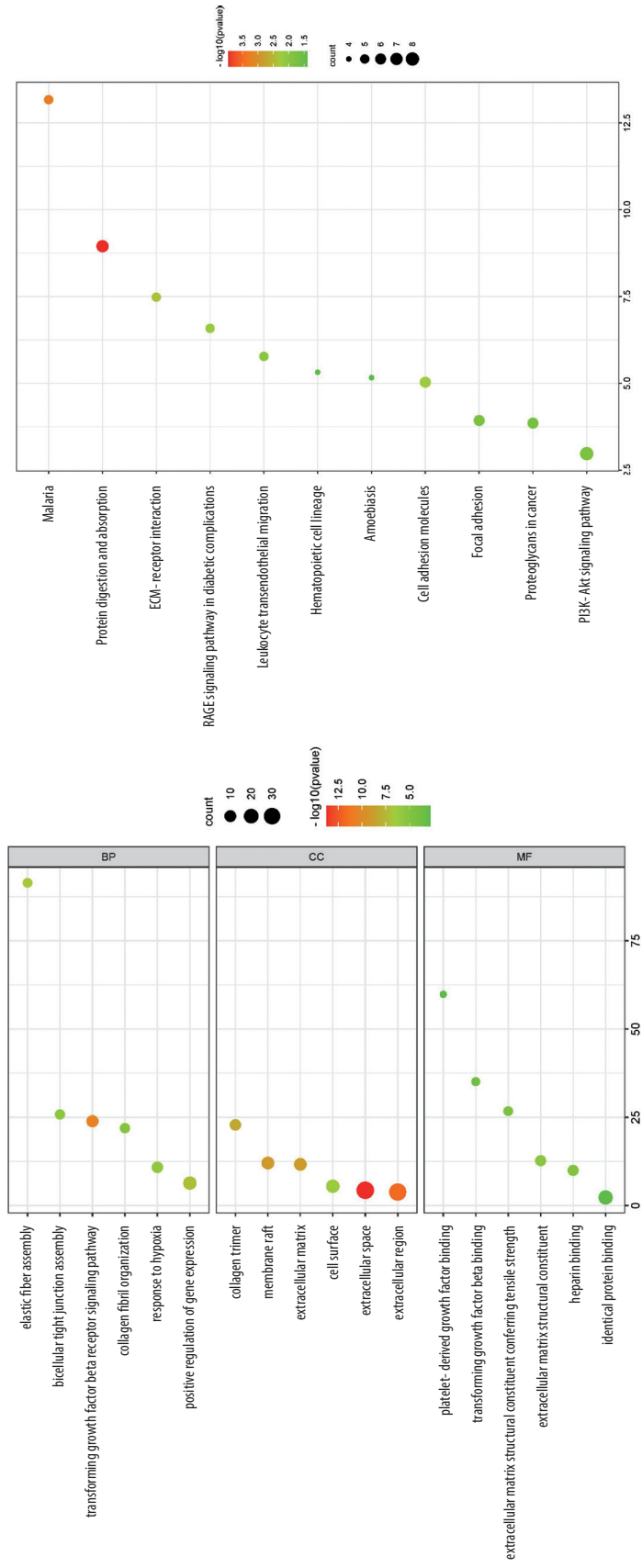


Figure 2. GO and KEGG enrichment analyses of the overlapping DEGs. **A.** Bubble figure of the top six KEGG terms. The abscissa represents the KEGG term, and the ordinate represents each term's $-\log_{10}(p\text{-value})$ enrichment. **B.** Bubble figure of GO pathways. The abscissa represents the GO term, and the ordinate represents the $-\log_{10}(p\text{-value})$ enrichment of each term.

immune infiltration revealed that *ANGPT1* expression was positively associated with the CD8+T cell infiltration level in various cancers, particularly in PAAD, THCA and LUSC (Fig. 5B). Next, the connections between the expression of *ANGPT1* and tumour immune infiltration in LUAD were further investigated. The findings showed that *ANGPT1* expression had a weak negative relationship with tumour purity and a significant correlation with the infiltration levels of B cells, CD8+T cells, CD4+T cells, macrophages, neutrophils and dendritic cells (Fig. 5C). This indicates that *ANGPT1* is closely related to immune regulation in LUAD.

Validating the mRNA expression levels of the hub genes in lung cancer

BEAS-2B, A549 and H1299 cells were chosen for further study. The mRNA expression levels of *ANGPT1*, *CDH5* and *CLDN5* were dramatically decreased in A549 cells and H1299 cells compared with BEAS-2B cells (Fig. 6A–C). In contrast, *COL3A1* expression was significantly increased (Fig. 6D). The mRNA expression levels of the four hub genes in LUAD were consistent with the previous results obtained by bioinformatics analysis.

ANGPT1 promotes the polarization of M1 macrophages in LUAD

The immuno-infiltration analysis showed a significant positive association between the mRNA expression of *ANGPT1* and macrophage infiltration in LUAD. To examine the function of *ANGPT1* in the regulation of macrophage cells, a co-culture system of A549 cells, H1299 cells and macrophages (M0) was constructed. The qRT-PCR results demonstrated that the mRNA expression levels of *NOX2* and *TNF- α* were dramatically lower in A549 cells than in M0 cells. When macrophages were co-cultured with A549 cells overexpressing *ANGPT1*, the mRNA expression levels of *NOX2* and *TNF- α* were substantially higher than in untreated A549 cells. Similar results were obtained in H1299 cells (Fig. 7A). The mRNA expression levels of *ARG1* and *IL-10*, both indicators of M2 macrophages, were significantly higher in A549 and H1299 cells co-cultured with M0 cells than in M0 cells. When A549 and H1299 cells were grown with macrophages and overexpressed *ANGPT1*, the *ARG1* and *IL-10* expression levels were lower than in untreated lung cancer cells (Fig. 7B). The Western blot results revealed that *iNOS* protein expression was increased in A549 and H1299 cells when *ANGPT1* was overexpressed. *CD206* pro-

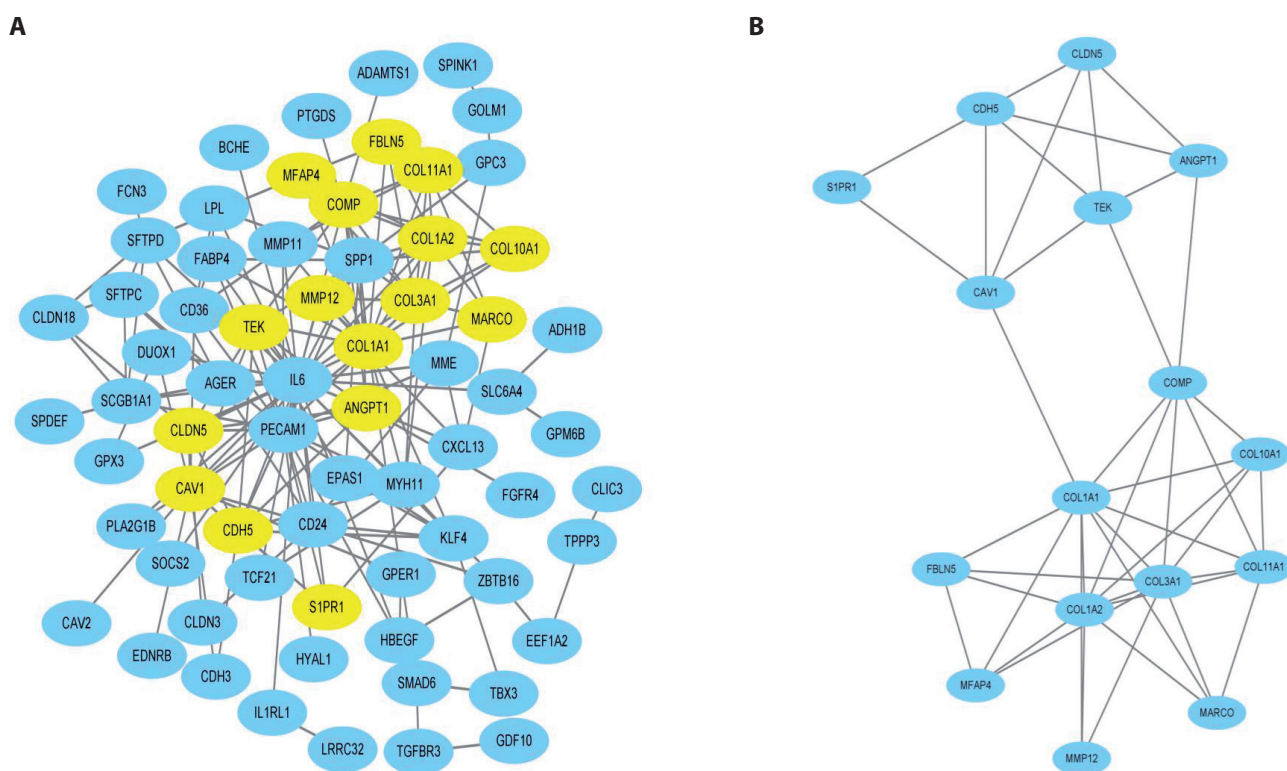
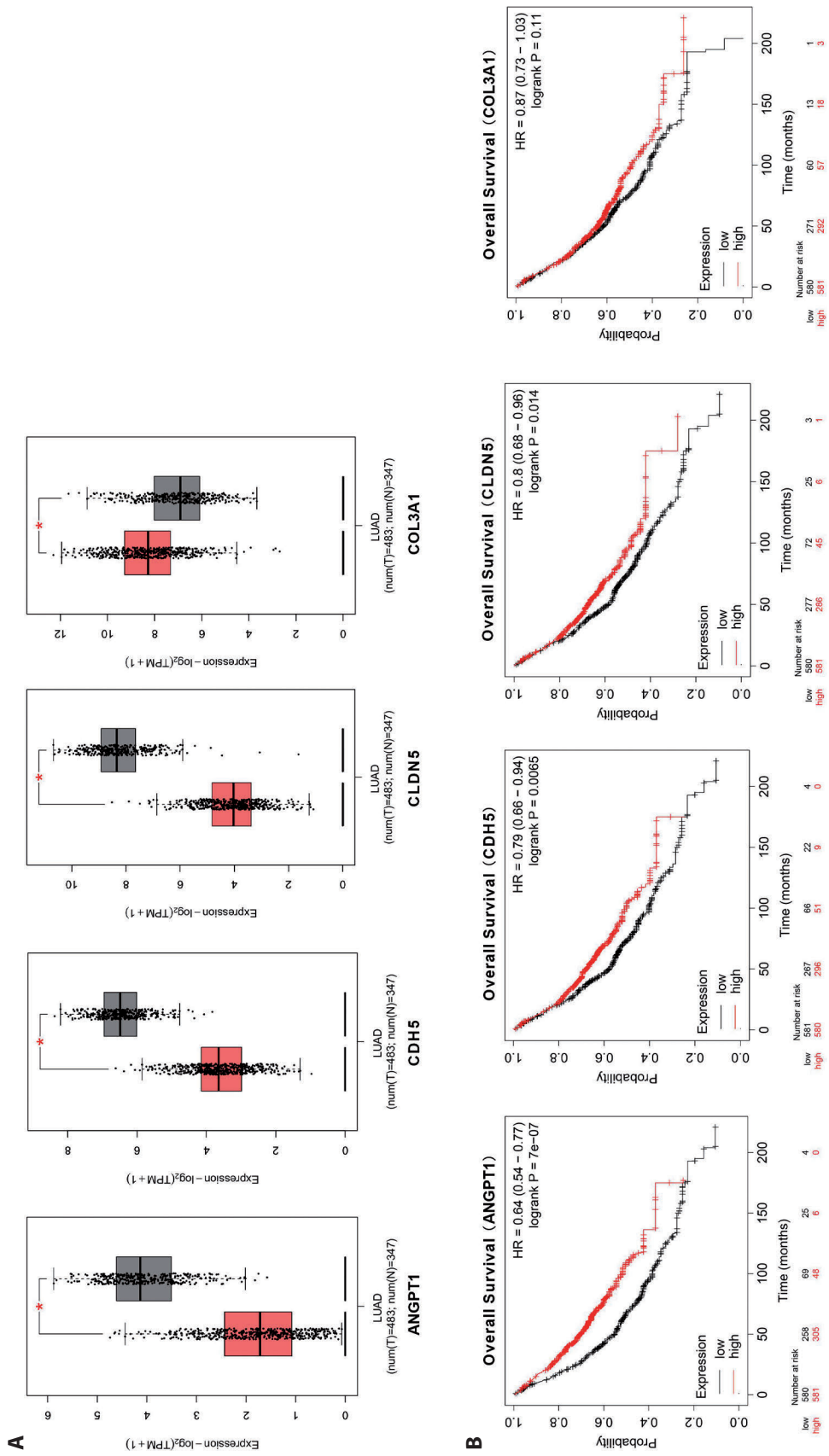


Figure 3. The hub modules were screened out by constructing a PPI network. **A.** Panoramic view of the PPI network. The genes marked in yellow represent the hub genes identified in the most important module based on the MCODE algorithm. **B.** The hub modules were determined using the MCODE plug-in in Cytoscape.



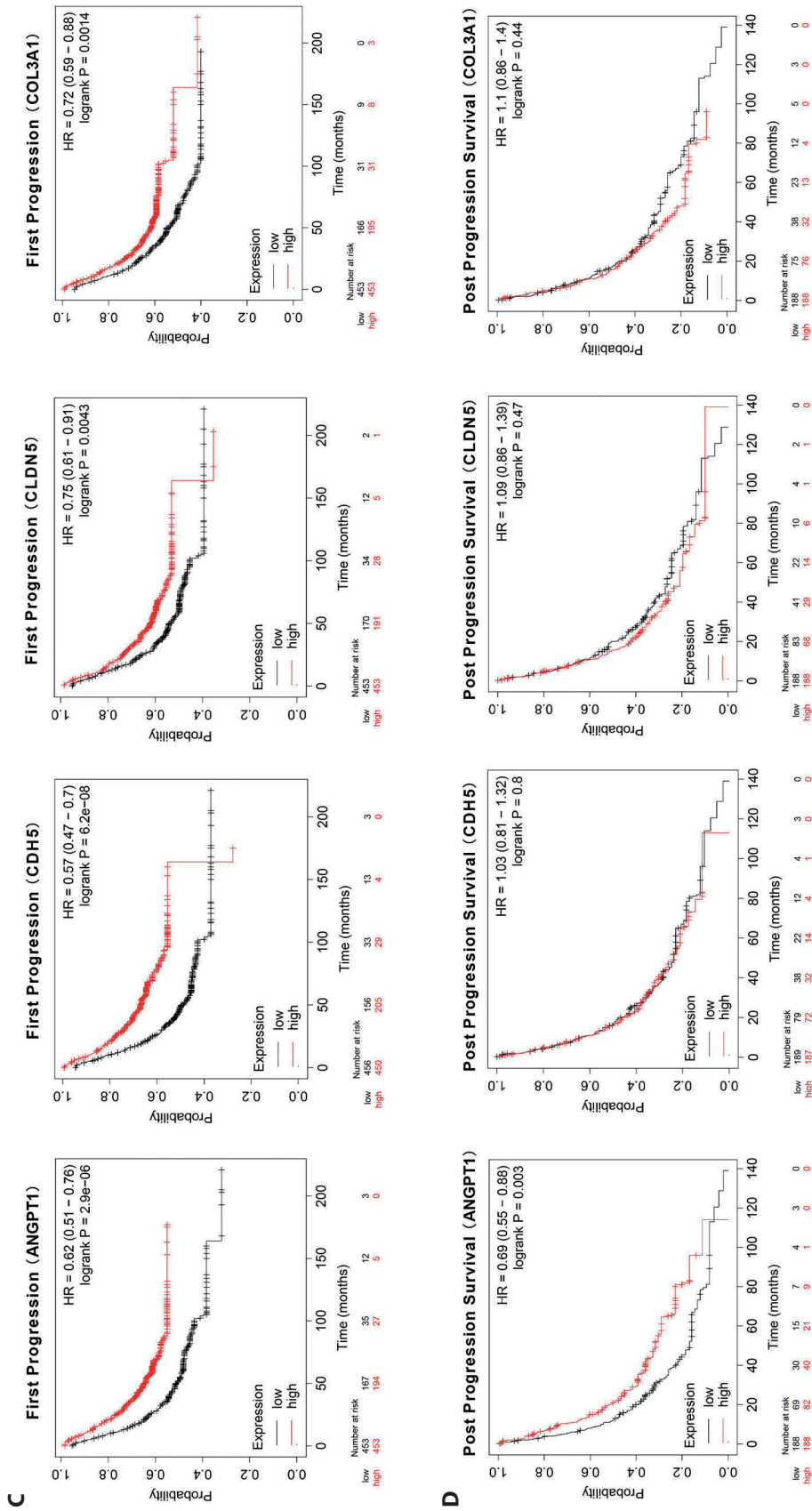


Figure 4. The mRNA expression and survival analysis of four hub genes. **A.** The mRNA expression of four hub genes: *ANGPT1*, *CDH5*, *CLDN5* and *COL3A1*. The overall **(B)**, first progression **(C)** and post-progression **(D)** survival analysis of four hub genes.

tein expression was considerably decreased in comparison to untreated LUAD cells (Fig. 7C).

ANGPT1 inhibits the progression of LUAD cells

After transfection, pcDNA-*ANGPT1* was overexpressed in A549 and H1299 cells. The significant increase in *ANGPT1* expression, as verified by RT-qPCR, confirmed the successful transfection (Fig. 8A). Functionally, *ANGPT1* was found to decrease the viability and inhibit the migration and invasion of both A549 and H1299 cells (Fig. 8B–D).

ANGPT1 inhibits the TGF- β signalling pathway in LUAD

To investigate the potential effect of *ANGPT1* on the TGF- β signalling pathway, Western blot analysis was performed. The findings demonstrated that transfection with pcDNA-*ANGPT1* significantly decreased the protein expression level of TGF- β , as well as the phosphorylation of *Smad2* and *Smad3*, in comparison to the pcDNA-NC control group (Fig. 9). This suggests that *ANGPT1* might exert its effects by modulating the TGF- β signalling pathway.

ANGPT1 inhibits the progression of LUAD cells by suppressing the TGF- β signalling pathway

The CCK-8 assay, wound healing assay and transwell assay results demonstrated that overexpression of *ANGPT1* significantly inhibited A549 cell viability, migration and invasion. Conversely, the addition of SRI-011381, a TGF- β signalling pathway activator, effectively reversed these inhibitory effects (Fig. 10A–C). These findings suggest that *ANGPT1* suppresses the proliferation, migration and invasion of LUAD cells primarily *via* the TGF- β signalling pathway.

Discussion

In recent years, the contributions of the TME to cancer development, progression and metastasis have been increasingly recognized due to rapid developments in molecular biology and high-throughput sequencing technologies (Qian et al. 2020). Tumour-initiated inflammatory signalling leads to the infiltration of multiple immune cell types into the TME, such as TAMs, tumour-reactive lymphocytes and mast cells (Bronte et al. 2006). In this study, a total of 88 immune infiltration-related DEGs in LUAD were screened using the GEO, GeneCards, BioGPS and GeneHopper databases. The overexpression of the hub genes *ANGPT1*, *CDH5* and *CLDN5* in LUAD was confirmed by RT-qPCR, whereas *COL3A1* expression was reduced. *ANGPT1* expression was found to be significantly correlated with OS, FP and PPS in LUAD. *ANGPT1* promoted M1 macrophage polarization

but inhibited M2 macrophage polarization. Furthermore, *ANGPT1* inhibited the proliferation, migration and invasion of LUAD by inhibiting the TGF- β signalling pathway.

We performed functional enrichment analysis of 88 overlapping immune infiltration-associated DEGs. KEGG enrichment analysis showed that immune infiltration-associated DEGs in LUAD were mainly associated with the malaria, protein digestion and absorption, and ECM receptor interaction, which is consistent with previous studies (Guo et al. 2019; Dai JJ et al. 2020; Niland et al. 2021). Inflammatory cytokines associated with a variety of cancers are affected by the Duffy antigen protein variant, which is induced by long-term exposure to malaria (Michon et al. 2001). Moreover, malaria infection may regulate immune checkpoint molecules (Butler et al. 2011). Current studies have revealed that the incidence of malaria is significantly correlated with endemic Burkitt lymphoma, colorectum and anus, colon, lung, stomach, and breast cancers (Qin et al. 2017; Redmond et al. 2020). Proteins provide nutrition for rapid tumor growth and proliferation. In advanced cancers, patients may develop malnutrition and cancer cachexia, which includes changes in protein metabolism (Gangadharan et al. 2017). Proteins such as collagen, fibronectin, and laminin are commonly found in the ECM, and alterations in their deposition can influence tumor progression (Fisseler-Eckhoff et al. 1990). In addition, ECM-receptor interactions are involved in a variety of tumor-related biological processes, including adhesion, degradation, mobility and proliferation (Zheng et al. 2021). Combining the above analyses, we hypothesize that immune infiltration-associated DEGs in LUAD may be involved in LUAD development through these pathways.

Advancements in bioinformatics have led to accumulating evidence highlighting the pivotal role of immune infiltration in the development of LUAD. One study identified a prognostic immune-cell characteristic score in LUAD through a pan-cancer analysis of immune cell infiltration (Zuo et al. 2020). Moreover, a multitude of immune infiltration-related genes have been found to influence LUAD tumour progression. For instance, *GREB1L*, associated with immune cell infiltration and highly expressed in LUAD, as well as *PD-1* and *PD-L1*, predict poor survival (Yu et al. 2021). *AMICA1*, identified as both a diagnostic and prognostic biomarker in LUAD, induces immune cell infiltration by activating the cGAS-STING signalling pathway (Feng et al. 2022). *GPI* is correlated with prognosis and immune infiltration and may serve as a prognostic biomarker in LUAD (Han et al. 2021). In this study, four immune infiltration-related key genes in LUAD were identified, namely, *ANGPT1*, *CDH5*, *CLDN5* and *COL3A1*. Among them, *ANGPT1*, *CDH5* and *CLDN5* exhibited low expression in LUAD while *COL3A1* was overexpressed. Consistent with the current findings, one study reported low expression of *CDH5* in LUAD (Fei et al. 2020). In addition, *CDH5* can be

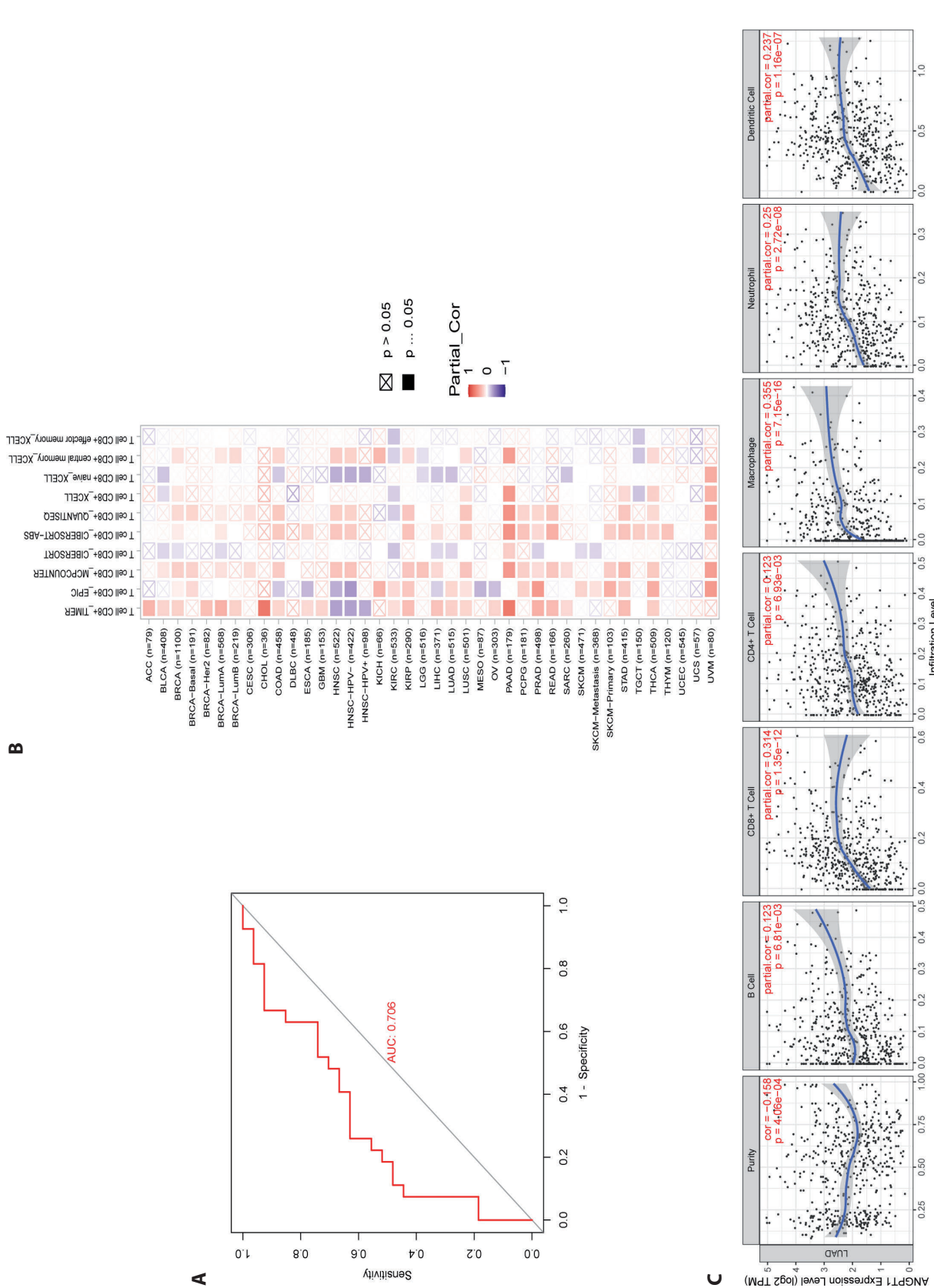


Figure 5. ROC curves and immune infiltration analysis of *ANGPT1*. **A.** ROC curves for the survival of *ANGPT1* in lung cancer. **B.** Association between *ANGPT1* expression and CD8+T cell immune infiltration in different tumours. **C.** Correlation analysis between *ANGPT1* expression and immune infiltration in LUAD.

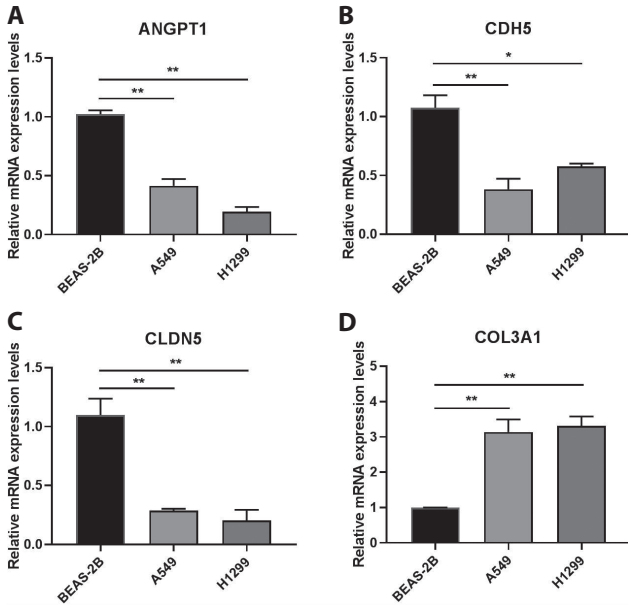


Figure 6. RT-qPCR was performed to detect the mRNA expression levels of four hub genes *ANGPT1* (A), *CDH5* (B), *CLDN5* (C), and *COL3A1* (D) in BEAS-2B cells, A549 cells and H1299 cells. * $p < 0.05$, ** $p < 0.01$ vs. BEAS-2B group.

used as a biomarker for non-small cell lung cancer and is associated with non-smoking female lung cancer patients (Shi et al. 2019; Obermayr et al. 2021). *CLDN5* exhibits low expression in lung squamous cell carcinoma and inhibits Akt phosphorylation-mediated proliferation (Akizuki et al. 2017). Moreover, it can inhibit lung cancer metastasis by regulating blood-brain barrier permeability (Ma et al. 2017). In the present study, low expression of *CLDN5* was found in lung cancer. Based on the above findings, it can be speculated that *CLDN5* might be an oncogene in lung cancer. Consistent with the current findings, previous research has demonstrated that *COL3A1* is overexpressed in lung cancer and that overexpression of *COL3A1* is associated with poor prognosis and cisplatin resistance (Wang et al. 2022). Subsequently, we explored the functional and molecular mechanism of *ANGPT1* in LUAD.

ANGPT1, produced by perivascular wall cells, plays a crucial role in vascular homeostasis (Fagiani and Cristofori 2013). Human neutrophils, capable of responding against different pathogens, are the most abundant circulating leukocytes (Wigerblad et al. 2022). Several angiogenic factors, including *ANGPT1*, form an extracellular network of neutrophils that awakens dormant cancer cells and

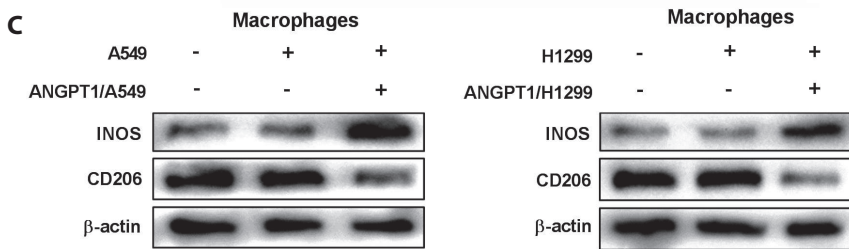
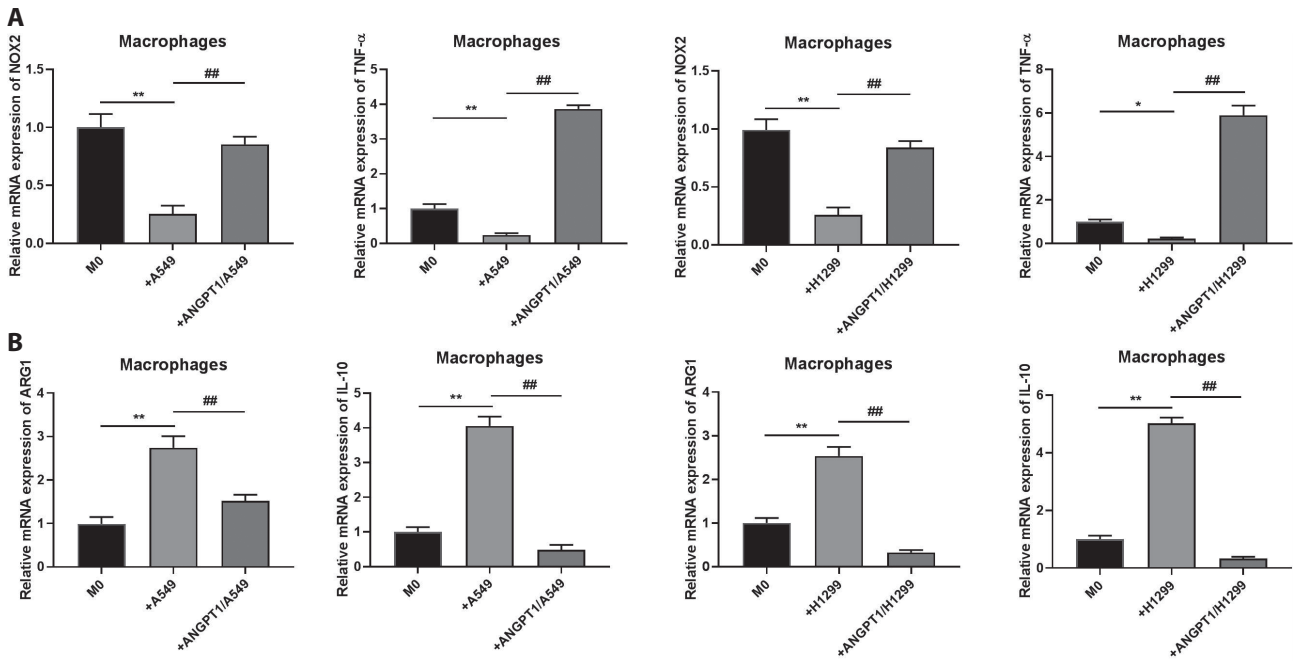


Figure 7. Analysis of the correlation between *ANGPT1* and M1 phenotype macrophages. RT-qPCR was performed to detect the mRNA expression of M1 (A) and M2 (B) macrophage markers. C. M1 and M2 marker proteins were detected using Western blot. * $p < 0.05$, ** $p < 0.01$ vs. M0 group; ## $p < 0.01$ vs. +A549/+H1299 group. M0, control.

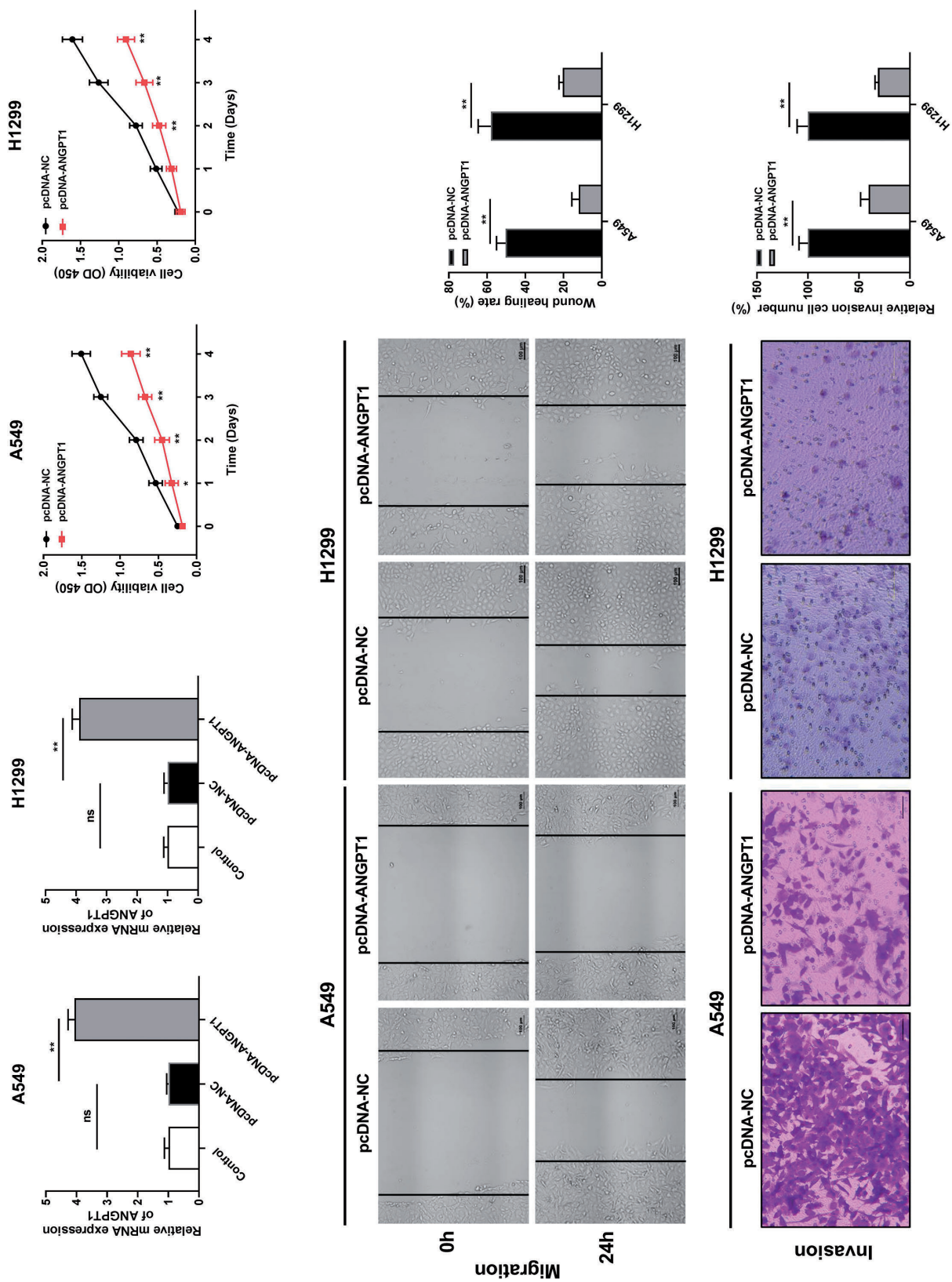


Figure 8. Effects of *ANGPT1* on the progression of LUAD cells. **A.** The transfection effect was verified by RT-qPCR. ** $p < 0.01$ vs. control group. Cell viability (**B**), cell migration ability (**C**) and cell invasion ability (**D**) were detected by CCK-8, wound healing, and transwell assays. * $p < 0.05$, ** $p < 0.01$ vs. pcDNA-NC group.

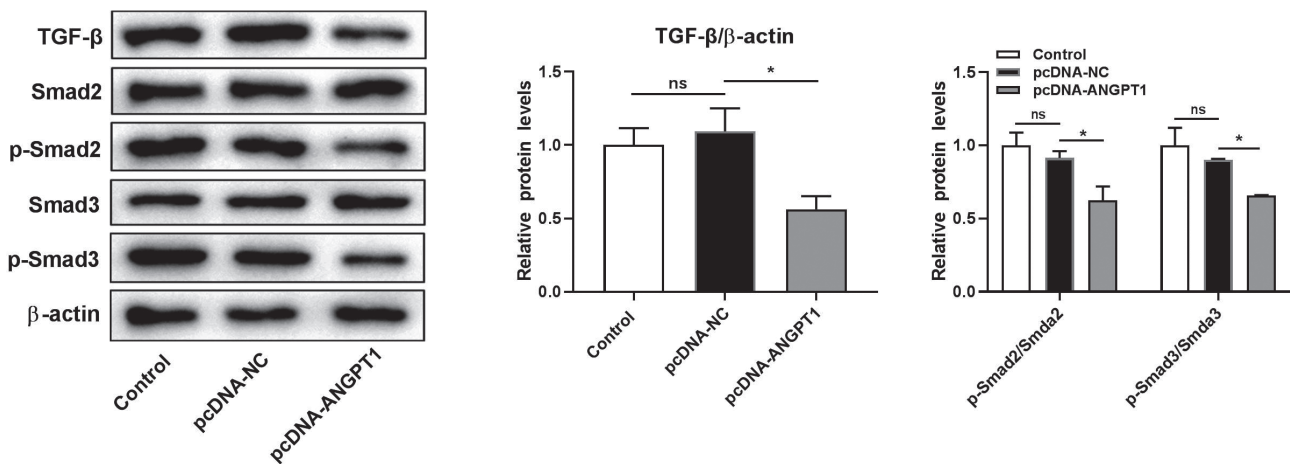


Figure 9. TGF- β signalling pathway-related protein expression after overexpression of *ANGPT1* was detected by Western blot. * $p < 0.05$ vs. pcDNA-NC group.

traps circulating tumor cells (Poto et al. 2022). Moreover, increased *ANGPT2*: *ANGPT1* ratio leads to destabilization of the tumor vasculature system, which reduce immune cell extravasation and tumor infiltration (Hakanpaa et al. 2015; Tian et al. 2017). *ANGPT1* is involved in the progression of multiple tumours. *ANGPT1* influences the timing of hematopoietic stem cell mobilization in patients with hematological malignancies and correlates with the number of circulating endothelial cells (Szmigielska-Kaplon et al. 2015). Serum levels of *ANGPT1* were significantly higher in patients with advanced nasopharyngeal carcinoma than that in early-stage disease progression (Guveli et al. 2016). In the ovarian cancer microenvironment, *ANGPT1* stimulate cancer cell proliferation and accumulate cancer-associated fibroblasts and tumour angiogenesis (Brunckhorst et al. 2014). In lung cancer, *ANGPT1* expression is downregulated and serves as a prognostic marker and potential tumour suppressor gene (Lu et al. 2021). Sex-specific SNP-SNP interaction analyses within topologically associated domains have revealed that *ANGPT1* expression is significantly downregulated in patients with squamous lung cancer and LUAD, and high expression of *ANGPT1* confers a higher survival probability (Yao et al. 2019). Consistent with previous studies, the current study also observed low expression of *ANGPT1* in LUAD, and an increased expression level of *ANGPT1* was indicative of a better prognosis in LUAD patients. In addition, the current study revealed that *ANGPT1* can reduce the proliferation and migration of A549 and H1299 cells by inhibiting the TGF- β signalling pathway. Therefore, it is speculated that *ANGPT1* might be a tumour suppressor gene in LUAD.

In the current study, immune infiltration analysis using the TIMER 2.0 database revealed a strong positive relationship between *ANGPT1* and TAMs. Further, *ANGPT1*

promoted the polarization of M1 macrophages but inhibited the polarization of M2 macrophages. TAMs are a significant type of immune cell that infiltrate the TME; they can be broadly classified into M1 macrophages and M2 macrophages (Pan et al. 2020). M1 macrophages are activated by IFN- γ and lipopolysaccharide, express IL-12, and mediate anti-tumour responses. M2 macrophages are activated by IL-4, IL-13 and IL-10, express IL-10, and promote tumour development by suppressing anti-tumour T cell responses (Ostrand-Rosenberg et al. 2012). Previous research has shown that *ANGPT1* is mainly expressed in macrophages (Nourhaghighi et al. 2003) and promotes the expression of the M1 phenotype macrophage markers *iNOS* and *CD86*, leading to increased atherosclerosis (Ou et al. 2020). This is consistent with the results of the current study. Therefore, considering the above findings together with the current findings, it can be speculated that *ANGPT1* likely inhibits LUAD tumour progression by promoting the polarization of M1 macrophages and inhibiting the polarization of M2 macrophages.

In summary, *ANGPT1* holds promise as a predictive marker for LUAD and shows potential in promoting the polarization of M1 macrophages. This study demonstrated that *ANGPT1* impedes the progression of LUAD by suppressing the TGF- β signalling pathway. Thus, *ANGPT1* may serve as a novel prognostic marker for LUAD and a potential target for immunotherapeutic strategies. However, this study is not without limitations. First, while several hub genes were identified through bioinformatics analysis, this study only explored the role and mechanism of *ANGPT1* in LUAD. Additionally, due to resource constraints, only *in vivo* experiments were performed. Despite these limitations, this research provides new insights into the immune mechanism of LUAD.

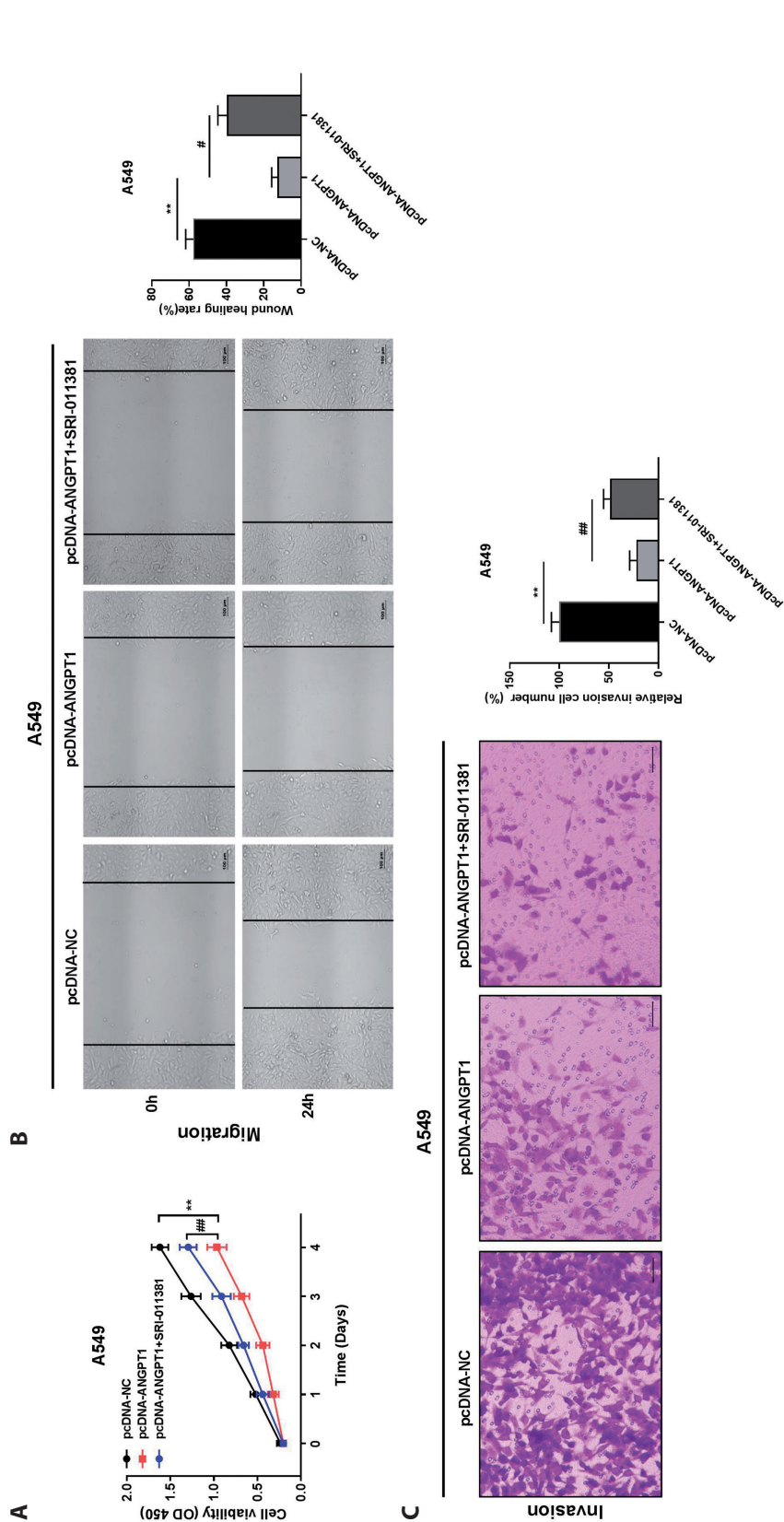


Figure 10. ANGPT1 inhibited the development of lung cancer cells by suppressing the TGF- β signalling pathway. Cell viability (A), cell migration ability (B) and cell invasion ability (C) were detected by CCK-8, wound healing and transwell assays, respectively. ** $p < 0.05$ vs. pcDNA-NC group; # $p < 0.05$, ## $p < 0.01$ vs. pcDNA-ANGPT1 group.

Ethics approval and consent to participate. The animal experiments were approved by the ethics committee of The Affiliated Hospital of Xuzhou Medical University. All methods were carried out in accordance with relevant guidelines and regulations.

Availability of data and materials. All data can be obtained by contacting the corresponding author.

Competing interests. The authors declare that they have no competing interests.

Funding. This study was supported by Xuzhou Key Research and Development Program (Social Development) (KC22097).

Authors' contributions. GL conceived and designed the present study, drafted the article. GL and HZ performed the experiments, analyzed the data. HZ revised the article critically for important intellectual content. All authors read and approved the final manuscript.

References

- Akizuki R, Shimobaba S, Matsunaga T, Endo S, Ikari A (2017): Claudin-5, -7, and -18 suppress proliferation mediated by inhibition of phosphorylation of Akt in human lung squamous cell carcinoma. *Biochim. Biophys. Acta Mol. Cell. Res.* **1864**, 293-302 <https://doi.org/10.1016/j.bbamcr.2016.11.018>
- Amaral ML, Erikson GA, Shokhirev MN (2018): BART: bioinformatics array research tool. *BMC Bioinformatics* **19**, 296 <https://doi.org/10.1186/s12859-018-2308-x>
- Bronte V, Cingarlini S, Marigo I, De Santo C, Gallina G, Dolcetti L, Ugel S, Peranzoni E, Mandruzzato S, Zanovello P (2006): Leukocyte infiltration in cancer creates an unfavorable environment for antitumor immune responses: a novel target for therapeutic intervention. *Immunol. Invest.* **35**, 327-357 <https://doi.org/10.1080/08820130600754994>
- Brunckhorst MK, Xu Y, Lu R, Yu Q (2014): Angiopoietins promote ovarian cancer progression by establishing a pro-cancer micro-environment. *Am. J. Pathol.* **184**, 2285-2296 <https://doi.org/10.1016/j.ajpath.2014.05.006>
- Butler NS, Moebius J, Pewe LL, Traore B, Doumbo OK, Tygrett LT, Waldschmidt TJ, Crompton PD, Harty JT (2011): Therapeutic blockade of PD-L1 and LAG-3 rapidly clears established blood-stage Plasmodium infection. *Nat. Immunol.* **13**, 188-195 <https://doi.org/10.1038/ni.2180>
- Chen Y, Zhao B, Wang X (2020): Tumor infiltrating immune cells (TIICs) as a biomarker for prognosis benefits in patients with osteosarcoma. *BMC Cancer* **20**, 1022 <https://doi.org/10.1186/s12885-020-07536-3>
- Dai JJ, Zhou WB, Wang B (2020): Identification of crucial genes associated with lung adenocarcinoma by bioinformatic analysis. *Medicine (Baltimore)* **99**, e23052 <https://doi.org/10.1097/MD.00000000000023052>
- Dai X, Lu L, Deng S, Meng J, Wan C, Huang J, Sun Y, Hu Y, Wu B, Wu G, et al. (2020): USP7 targeting modulates anti-tumor immune response by reprogramming Tumor-associated macrophages in lung cancer. *Theranostics* **10**, 9332-9347 <https://doi.org/10.7150/thno.47137>
- Fagiani E, Christofori G (2013): Angiopoietins in angiogenesis. *Cancer Lett.* **328**, 18-26 <https://doi.org/10.1016/j.canlet.2012.08.018>
- Fei H, Chen S, Xu C (2020): Interactive verification analysis of multiple sequencing data for identifying potential biomarker of lung adenocarcinoma. *Biomed. Res. Int.* **2020**, 8931419 <https://doi.org/10.1155/2020/8931419>
- Feng Z, Zhang Y, He M, Han Y, Cai C, Liu S, Liu P, Chen Y, Shen H, Zeng S (2022): AMICA1 is a diagnostic and prognostic biomarker and induces immune cells infiltration by activating cGAS-STING signaling in lung adenocarcinoma. *Cancer Cell. Int.* **22**, 111 <https://doi.org/10.1186/s12935-022-02517-x>
- Fisseler-Eckhoff A, Prebeg M, Voss B, Müller K (1990): Extracellular matrix in preneoplastic lesions and early cancer of the lung. *Pathol. Res. Pract.* **186**, 95-101 [https://doi.org/10.1016/S0344-0338\(11\)81016-2](https://doi.org/10.1016/S0344-0338(11)81016-2)
- Gangadharan A, Choi SE, Hassan A, Ayoub NM, Durante G, Balwani S, Kim YH, Pecora A, Goy A, Suh KS (2017): Protein calorie malnutrition, nutritional intervention and personalized cancer care. *Oncotarget* **8**, 24009-24030 <https://doi.org/10.18632/oncotarget.15103>
- Grenga I, Kwilas AR, Donahue RN, Farsaci B, Hodge JW (2015): Inhibition of the angiopoietin/Tie2 axis induces immunogenic modulation, which sensitizes human tumor cells to immune attack. *J. Immunother. Cancer* **3**, 52 <https://doi.org/10.1186/s40425-015-0096-7>
- Guo T, Ma H, Zhou Y (2019): Bioinformatics analysis of microarray data to identify the candidate biomarkers of lung adenocarcinoma. *PeerJ* **7**, e7313 <https://doi.org/10.7717/peerj.7313>
- Guveli ME, Duranyildiz D, Karadeniz A, Bilgin E, Serilmez M, Soyuncu HO, Yasasever V (2016): Circulating serum levels of angiopoietin-1 and angiopoietin-2 in nasopharynx and larynx carcinoma patients. *Tumour Biol.* **37**, 8979-8983 <https://doi.org/10.1007/s13277-015-4777-0>
- Gyorffy B, Surowiak P, Budczies J, Lanczky A (2013): Online survival analysis software to assess the prognostic value of biomarkers using transcriptomic data in non-small-cell lung cancer. *PLoS One* **8**, e82241 <https://doi.org/10.1371/journal.pone.0082241>
- Hakanpää L, Sipilä T, Leppänen VM, Gautam P, Nurmi H, Jacquemet G, Eklund L, Ivaska J, Alitalo K, Saharinen P (2015): Endothelial destabilization by angiopoietin-2 via integrin beta1 activation. *Nat. Commun.* **6**, 5962 <https://doi.org/10.1038/ncomms6962>
- Han J, Deng X, Sun R, Luo M, Liang M, Gu B, Zhang T, Peng Z, Lu Y, Tian C, et al. (2021): GPI is a prognostic biomarker and correlates with immune infiltrates in lung adenocarcinoma. *Front. Oncol.* **11**, 752642 <https://doi.org/10.3389/fonc.2021.752642>
- Hawighorst T, Skobe M, Streit M, Hong YK, Velasco P, Brown LF, Riccardi L, Lange-Asschenfeldt B, Detmar M (2002): Activation of the tie2 receptor by angiopoietin-1 enhances tumor vessel maturation and impairs squamous cell carcinoma growth. *Am. J. Pathol.* **160**, 1381-1392 [https://doi.org/10.1016/S0002-9440\(10\)62565-5](https://doi.org/10.1016/S0002-9440(10)62565-5)

- Hutchinson BD, Shroff GS, Truong MT, Ko JP (2019): Spectrum of lung adenocarcinoma. *Semin. Ultrasound CT MR* **40**, 255-264
<https://doi.org/10.1053/j.sult.2018.11.009>
- Jayson GC, Kerbel R, Ellis LM, Harris AL (2016): Antiangiogenic therapy in oncology: current status and future directions. *Lancet* **388**, 518-529
[https://doi.org/10.1016/S0140-6736\(15\)01088-0](https://doi.org/10.1016/S0140-6736(15)01088-0)
- Jurisc V, Vukovic V, Obradovic J, Gulyaeva LF, Kushlinskii NE, Djordjevic N (2020): EGFR polymorphism and survival of NSCLC patients treated with TKIs: A systematic review and meta-analysis. *J. Oncol.* **2020**, 1973241
<https://doi.org/10.1155/2020/1973241>
- Liu Y, Xu R, Gu H, Zhang E, Qu J, Cao W, Huang X, Yan H, He J, Cai Z (2021): Metabolic reprogramming in macrophage responses. *Biomark. Res.* **9**, 1
<https://doi.org/10.1186/s40364-020-00251-y>
- Liu M, Fan X, Liao W, Li Y, Ma L, Yuan M, Gu R, Wei Z, Wang C, Zhang H (2021): Identification of significant genes as prognostic markers and potential tumor suppressors in lung adenocarcinoma via bioinformatical analysis. *BMC Cancer* **21**, 616
<https://doi.org/10.1186/s12885-021-08308-3>
- Ma SC, Li Q, Peng JY, Zhouwen JL, Diao JF, Niu JX, Wang X, Guan XD, Jia W, Jiang WG (2017): Claudin-5 regulates blood-brain barrier permeability by modifying brain microvascular endothelial cell proliferation, migration, and adhesion to prevent lung cancer metastasis. *CNS Neurosci. Ther.* **23**, 947-960
<https://doi.org/10.1111/cns.12764>
- Michon P, Woolley I, Wood EM, Kastens W, Zimmerman PA, Adams JH (2001): Duffy-null promoter heterozygosity reduces DARC expression and abrogates adhesion of the *P. vivax* ligand required for blood-stage infection. *FEBS Lett.* **495**, 111-114
[https://doi.org/10.1016/S0014-5793\(01\)02370-5](https://doi.org/10.1016/S0014-5793(01)02370-5)
- Niland S, Riscanevo AX, Eble JA (2021): Matrix metalloproteinases shape the tumor microenvironment in cancer progression. *Int. J. Mol. Sci.* **23**, 146
<https://doi.org/10.3390/ijms23010146>
- Nourhaghghi N, Teichert-Kuliszewska K, Davis J, Stewart DJ, Nag S (2003): Altered expression of angiopoietins during blood-brain barrier breakdown and angiogenesis. *Lab. Invest.* **83**, 1211-1222
<https://doi.org/10.1097/01.LAB.0000082383.40635.FE>
- Obermayr E, Koppensteiner N, Heinzl N, Schuster E, Holzer B, Fabikan H, Weinlinger C, Illini O, Hochmair M, Zeillinger R (2021): Cancer stem cell-like circulating tumor cells are prognostic in non-small cell lung cancer. *J. Pers. Med.* **11**, 1225
<https://doi.org/10.3390/jpm11111225>
- Ostrand-Rosenberg S, Sinha P, Beury DW, Clements VK (2012): Cross-talk between myeloid-derived suppressor cells (MDSC), macrophages, and dendritic cells enhances tumor-induced immune suppression. *Semin. Cancer Biol.* **22**, 275-281
<https://doi.org/10.1016/j.semcancer.2012.01.011>
- Ou X, Gao JH, He LH, Yu XH, Wang G, Zou J, Zhao ZW, Zhang DW, Zhou ZJ, Tang CK (2020): Angiopoietin-1 aggravates atherosclerosis by inhibiting cholesterol efflux and promoting inflammatory response. *Biochim. Biophys. Acta Mol. Cell. Biol. Lipids* **1865**, 158535
<https://doi.org/10.1016/j.bbalip.2019.158535>
- Pan Y, Yu Y, Wang X, Zhang T (2020): Tumor-associated macrophages in tumor immunity. *Front. Immunol.* **11**, 583084
<https://doi.org/10.3389/fimmu.2020.583084>
- Poto R, Cristinziano L, Modestino L, de Paulis A, Marone G, Loffredo S, Galdiero MR, Varricchi G (2022): Neutrophil extracellular traps, angiogenesis and cancer. *Biomedicines* **10**, 431
<https://doi.org/10.3390/biomedicines10020431>
- Qian J, Olbrecht S, Boeckx B, Vos H, Laoui D, Etlioglu E, Wauters E, Pomella V, Verbandt S, Busschaert P, et al. (2020): A pan-cancer blueprint of the heterogeneous tumor microenvironment revealed by single-cell profiling. *Cell. Res.* **30**, 745-762
<https://doi.org/10.1038/s41422-020-0355-0>
- Qin L, Chen C, Chen L, Xue R, Ou-Yang M, Zhou C, Zhao S, He Z, Xia Y, He J, et al. (2017): Worldwide malaria incidence and cancer mortality are inversely associated. *Infect. Agent. Cancer* **12**, 14
<https://doi.org/10.1186/s13027-017-0117-x>
- Redmond LS, Ogowang MD, Kerchan P, Reynolds SJ, Tenge CN, Were PA, Kuremu RT, Masalu N, Kawira E, Otim I, et al. (2020): Endemic Burkitt lymphoma: a complication of asymptomatic malaria in sub-Saharan Africa based on published literature and primary data from Uganda, Tanzania, and Kenya. *Malar. J.* **19**, 239
<https://doi.org/10.1186/s12936-020-03312-7>
- Shi K, Li N, Yang M, Li W (2019): Identification of key genes and pathways in female lung cancer patients who never smoked by a bioinformatics analysis. *J. Cancer* **10**, 51-60
<https://doi.org/10.7150/jca.26908>
- Spella M, Stathopoulos GT (2021): Immune resistance in lung adenocarcinoma. *Cancers (Basel)* **13**, 384
<https://doi.org/10.3390/cancers13030384>
- Suri C, Jones PF, Patan S, Bartunkova S, Maisonpierre PC, Davis S, Sato TN, Yancopoulos GD (1996): Requisite role of angiopoietin-1, a ligand for the TIE2 receptor, during embryonic angiogenesis. *Cell* **87**, 1171-1180
[https://doi.org/10.1016/S0092-8674\(00\)81813-9](https://doi.org/10.1016/S0092-8674(00)81813-9)
- Szmigielska-Kaplon A, Krawczynska A, Czemerska M, Pluta A, Cebula-Obrzut B, Szmigielska K, Stepka K, Smolewski P, Robak T, Wierzbowska A (2015): Angiopoietins in haematopoietic stem cell mobilisation in patients with haematological malignancies. *Blood Transfus.* **13**, 102-108
- Tian L, Goldstein A, Wang H, Ching Lo H, Sun Kim I, Welte T, Sheng K, Dobrolecki LE, Zhang X, Putluri N, et al. (2017): Mutual regulation of tumour vessel normalization and immunostimulatory reprogramming. *Nature* **544**, 250-254
<https://doi.org/10.1038/nature21724>
- Travis WD, Brambilla E, Noguchi M, Nicholson AG, Geisinger K, Yatabe Y, Powell CA, Beer D, Riely G, Garg K, et al. (2011): International Association for the Study of Lung Cancer/American Thoracic Society/European Respiratory Society: international multidisciplinary classification of lung adenocarcinoma: executive summary. *Proc. Am. Thorac. Soc.* **8**, 381-385
<https://doi.org/10.1513/pats.201107-042ST>
- Wang L, Sun Y, Guo Z, Liu H (2022): COL3A1 overexpression associates with poor prognosis and cisplatin resistance in lung cancer. *Balkan Med. J.* **39**, 393-400
<https://doi.org/10.4274/balkanmedj.galenos.2022.2022-6-16>
- Wen H, Chen H, Xie L, Li Z, Zhang Q, Tian Q (2022): Macrophage-related molecular subtypes in lung adenocarcinoma identify

- novel tumor microenvironment with prognostic and therapeutic implications. *Front. Genet.* **13**, 1012164
<https://doi.org/10.3389/fgene.2022.1012164>
- Wigerblad G, Cao Q, Brooks S, Naz F, Gadkari M, Jiang K, Gupta S, O'Neil L, Dell'Orso S, Kaplan MJ, Franco LM (2022): Single-cell analysis reveals the range of transcriptional states of circulating human neutrophils. *J. Immunol.* **209**, 772-782
<https://doi.org/10.4049/jimmunol.2200154>
- Xu C, Song L, Yang Y, Liu Y, Pei D, Liu J, Guo J, Liu N, Li X, Liu Y, et al. (2022): Clinical M2 macrophage-related genes can serve as a reliable predictor of lung adenocarcinoma. *Front. Oncol.* **12**, 919899
<https://doi.org/10.3389/fonc.2022.919899>
- Yao S, Dong SS, Ding JM, Rong Y, Zhang YJ, Chen H, Chen JB, Chen YX, Yan H, Dai Z, Guo Y (2019): Sex-specific SNP-SNP interaction analyses within topologically associated domains reveals ANGPT1 as a novel tumor suppressor gene for lung cancer. *Genes Chromosomes Cancer* **59**, 13-22
<https://doi.org/10.1002/gcc.22793>
- Yu Y, Wang Z, Zheng Q, Li J (2021): GREB1L overexpression correlates with prognosis and immune cell infiltration in lung adenocarcinoma. *Sci. Rep.* **11**, 13281
<https://doi.org/10.1038/s41598-021-92695-x>
- Zhang C, Zhang J, Xu FP, Wang YG, Xie Z, Su J, Dong S, Nie Q, Shao Y, Zhou Q, et al. (2019): Genomic landscape and immune microenvironment features of preinvasive and early invasive lung adenocarcinoma. *J. Thorac. Oncol.* **14**, 1912-1923
<https://doi.org/10.1016/j.jtho.2019.07.031>
- Zhang H, Guo L, Chen J (2020): Rationale for lung adenocarcinoma prevention and drug development based on molecular biology during carcinogenesis. *Onco. Targets Ther.* **13**, 3085-3091
<https://doi.org/10.2147/OTT.S248436>
- Zheng Q, Min S, Zhou Q (2021): Identification of potential diagnostic and prognostic biomarkers for LUAD based on TCGA and GEO databases. *Biosci. Rep.* **41**, BSR20204370
<https://doi.org/10.1042/BSR20204370>
- Zuo S, Wei M, Wang S, Dong J, Wei J (2020): Pan-cancer analysis of immune cell infiltration identifies a prognostic immune-cell characteristic score (ICCS) in lung adenocarcinoma. *Front. Immunol.* **11**, 1218
<https://doi.org/10.3389/fimmu.2020.01218>

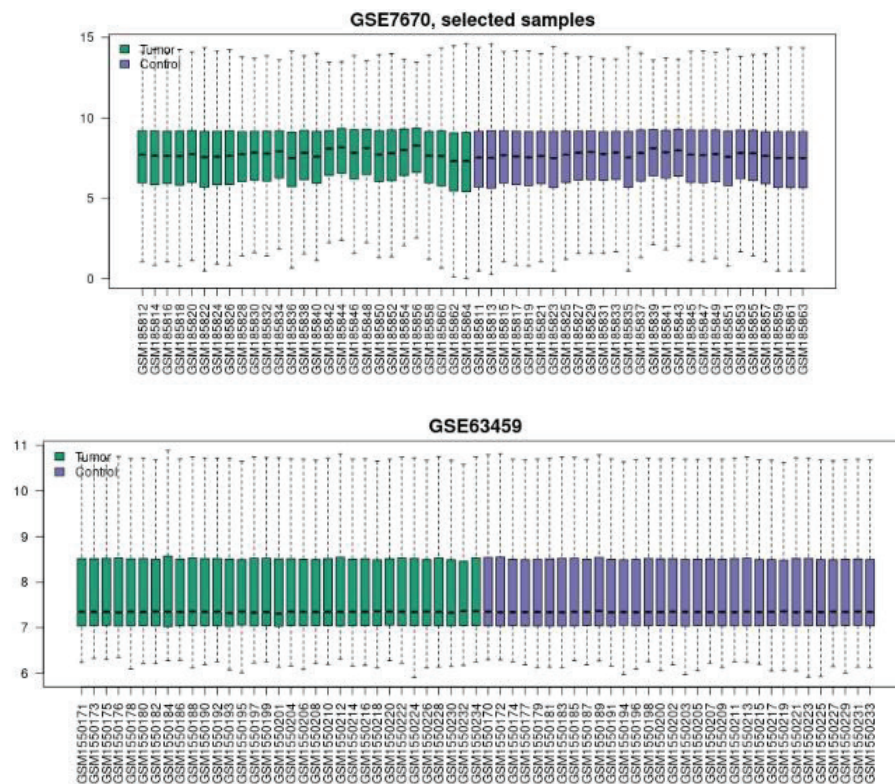
Received: August 3, 2023

Final version accepted: January 12, 2024

Supplementary Material

ANGPT1 promotes M1 macrophage polarization and inhibits lung adenocarcinoma progression by inhibiting the TGF- β signalling pathwayGang Liu^{1,2} and Hao Zhang^{1,3} ¹ Department of Thoracic Surgery, The Affiliated Hospital of Xuzhou Medical University, Xuzhou City, Jiangsu Province, China² Department of Thoracic Surgery, The Second Affiliated Hospital of Bengbu Medical University, Bengbu City, Anhui Province, China³ Thoracic Surgery Laboratory, Xuzhou Medical University, Xuzhou City, Jiangsu Province, China

Supplementary Figures

**Figure S1.** The read counts were normalized for each sample in both the GSE7670 and GSE63459 datasets.

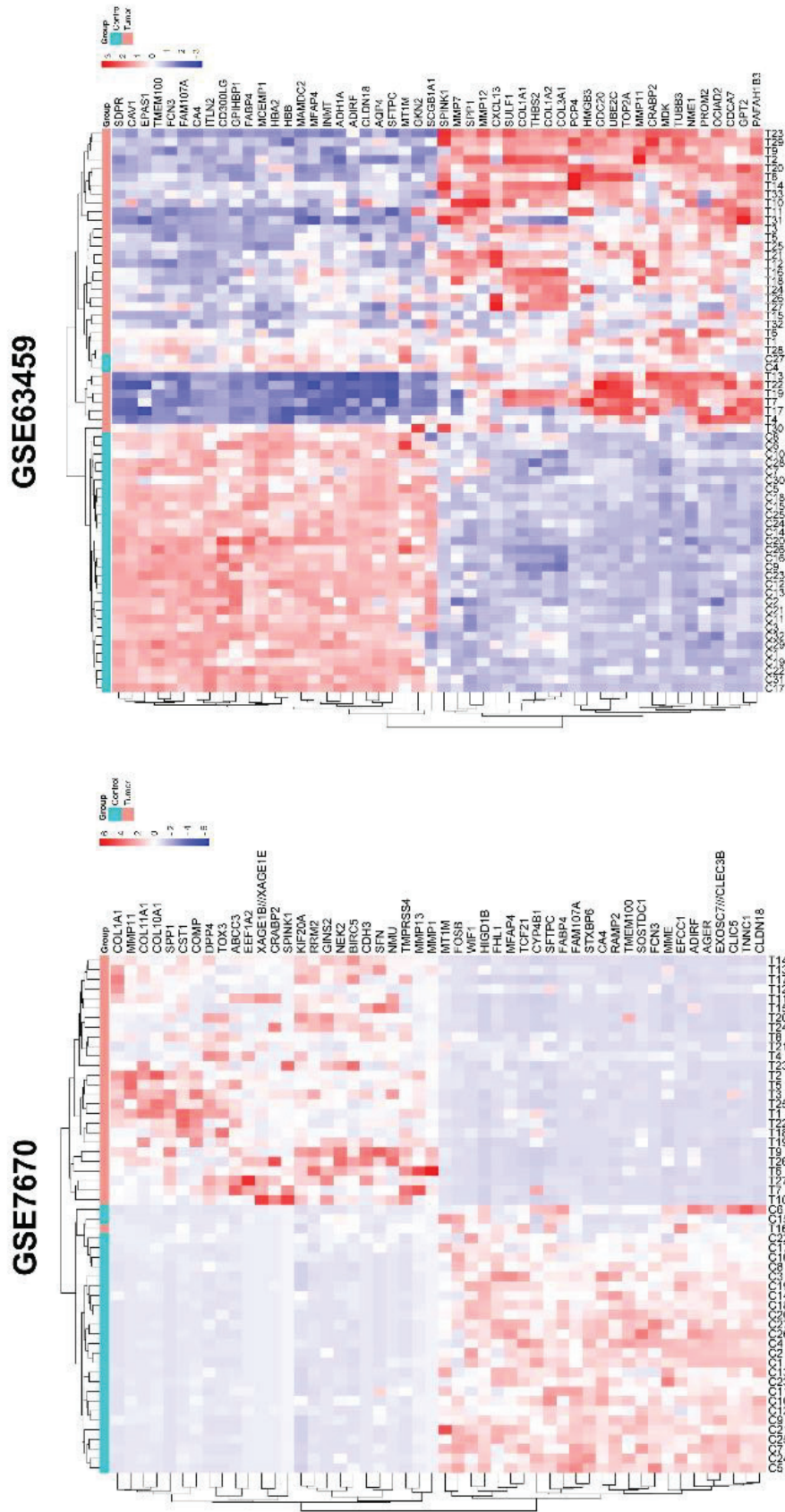


Figure S2. Heatmaps illustrating the expression patterns of the top 50 DEGs across all samples in the two datasets.

Venn Diagram

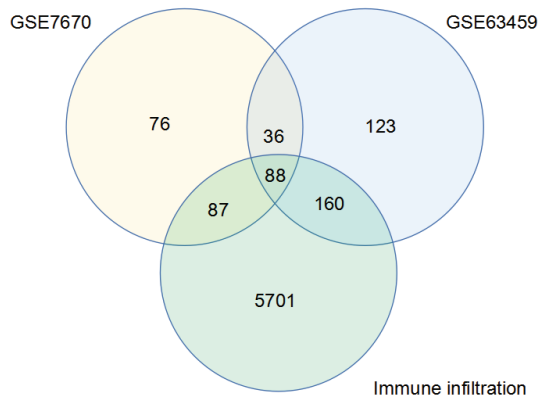


Figure S3. Venn diagram of immune infiltration-associated DEGs.

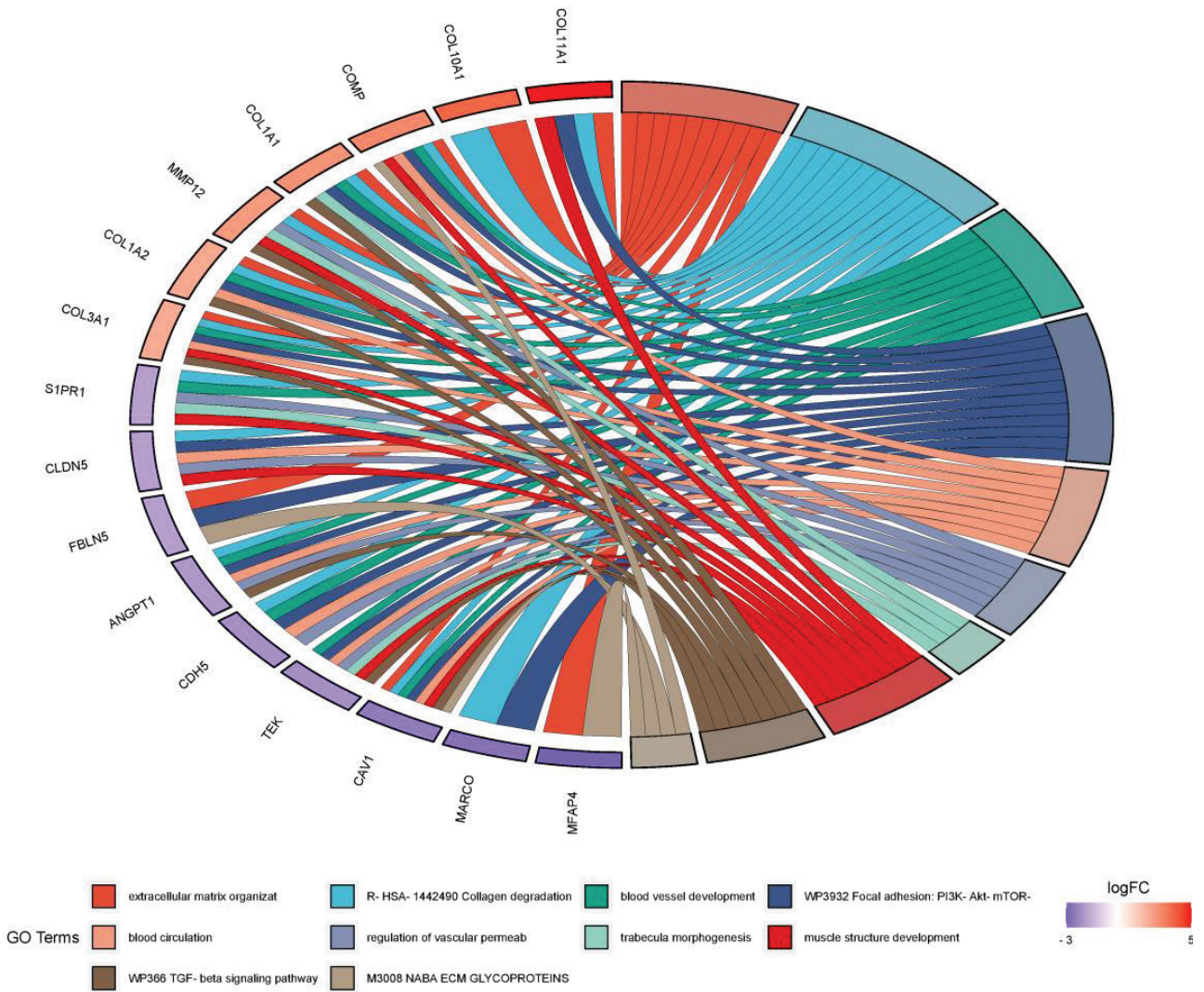


Figure S4. GO enrichment analysis of 16 hub genes.

Supplementary Tables

Table S1. Detailed information on the GEO microarray profiles of LUAD

No. of GEO profile	Type	Case	Control	Platform
GSE7670	mRNA	27 LUAD tissues	27 adjacent normal tissues	GPL96
GSE63459	mRNA	33 LUAD tissues	32 adjacent normal tissues	GPL6883

Table S2. The primer sequences

Primer name	Sequence (5'-3')
GAPDH-F	CCGGGAAACTGTGGCGTGATGG
GAPDH-R	AGGTGGAGGAGTGGGTGTCGCTGTT
ANGPT1-F	GAAGGGAACCGAGCCTATTC
ANGPT1-R	GGGCACATTTGCACATACAG
CDH5-F	CCTACCAGCCCAAAGTGTGT
CDH5-R	GACTTGGCATCCCATTTGTCT
CLDN5-F	GAGGCGTGCTCTACCTGTTT
CLDN5-R	GTACTTCACGGGGAAGCTGA
COL3A1-F	TACGGCAATCCTGAACTTCC
COL3A1-R	GTGTGTTTCGTGCAACCATC
NOX2-F	TCACTTCCTCCACCAAAACC
NOX2-R	GGGATTGGGCATTCCTTTAT
TNF- α -F	ACGGAGAAGAAGCAGACCAA
TNF- α -R	CGCAGTTCAAAGGTCTCCTC
ARG1-F	GGCTGGTCTGCTTGAGAAAC
ARG1-R	ATTGCCAAACTGTGGTCTCC
IL-10-F	TGGTGAAACCCCGTCTCTAC
IL-10-R	CTGGAGTACAGGGGCATGAT

Table S3. The top 20 DEGs in the GSE7670 and GSE63459 datasets

Gene	Description	<i>p</i> -adj	Up/Down
GSE7670			
COL11A1	Collagen type XI alpha 1 chain	1.21E-10	Up
MMP1	Matrix metalloproteinase 1	4.03E-09	Up
XAGE1B	X antigen family member 1B	6.04E-08	Up
CDH3	Cadherin 3	6.54E-11	Up
SPP1	Secreted phosphoprotein 1	2.03E-15	Up
SPINK1	Serine peptidase inhibitor, Kazal type 1	2.79E-06	Up
COL10A1	Collagen type X alpha 1 chain	4.31E-11	Up
TMPRSS4	Transmembrane protease, serine 4	3.05E-11	Up
ABCC3	ATP binding cassette subfamily C member 3	8.03E-11	Up
TOP2A	Topoisomerase (DNA) II alpha	3.96E-08	Up
AGER	Advanced glycosylation end-product specific receptor	3.81E-16	Down
FAM107A	Family with sequence similarity 107 member A	2.15E-14	Down
TNNC1	Troponin C1, slow skeletal and cardiac type	8.44E-13	Down
SFTPC	Surfactant protein C	4.04E-07	Down
AGER	Advanced glycosylation end-product specific receptor	1.55E-15	Down
SFTPC	Surfactant protein C	3.21E-07	Down
SFTPC	Surfactant protein C	2.02E-12	Down
WIF1	WNT inhibitory factor 1	3.71E-11	Down
CA4	Carbonic anhydrase 4	2.14E-15	Down
SOSTDC1	Sclerostin domain containing 1	1.11E-12	Down
GSE63459			
SPP1	Secreted phosphoprotein 1	1.38E-07	Up
COL1A1	Collagen type I alpha 1 chain	4.12E-10	Up
SPINK1	Serine peptidase inhibitor, Kazal type 1	1.00E-04	Up
TOP2A	Topoisomerase (DNA) II alpha	3.52E-10	Up
TUBB3	Tubulin beta 3 class III	1.54E-10	Up
MMP12	Matrix metalloproteinase 12	7.02E-08	Up
MDK	Midkine (neurite growth-promoting factor 2)	1.79E-12	Up
CRABP2	Cellular retinoic acid binding protein 2	1.62E-08	Up
UBE2C	Ubiquitin conjugating enzyme E2 C	2.46E-08	Up
HMGB3	High mobility group box 3	6.39E-08	Up
FCN3	Ficolin 3	6.01E-14	Down
CLDN18	Claudin 18	1.68E-12	Down
SFTPC	Surfactant protein C	1.95E-10	Down
MCEMP1	Mast cell expressed membrane protein 1	1.32E-18	Down
AGER	Advanced glycosylation end-product specific receptor	3.89E-19	Down
FAM107A	Family with sequence similarity 107 member A	1.03E-14	Down
HBA2	Hemoglobin subunit alpha 2	1.73E-14	Down
TMEM100	Transmembrane protein 100	1.96E-16	Down
ITLN2	Intelectin 2	2.44E-18	Down
CAV1	Caveolin 1	1.79E-15	Down